

# Efficient classical simulation of noisy quantum computation

Xun Gao<sup>1</sup> and Luming Duan<sup>1</sup>

<sup>1</sup>*Center for Quantum Information, IIS, Tsinghua University, Beijing 100084, PR China*

Understanding the boundary between classical simulatability and the power of quantum computation is a fascinating topic. Direct simulation of noisy quantum computation requires solving an open quantum many-body system, which is very costly. Here, we develop a tensor network formalism to simulate the time-dynamics and the Fourier spectrum of noisy quantum circuits. We prove that under general conditions most of the quantum circuits at any constant level of noise per gate can be efficiently simulated classically with the cost increasing only polynomially with the size of the circuits. The result holds even if we have perfect noiseless quantum gates for some subsets of operations, such as all the gates in the Clifford group. This surprising result reveals the subtle relations between classical simulatability, quantum supremacy, and fault-tolerant quantum computation. The developed simulation tools may also be useful for solving other open quantum many-body systems.

## INTRODUCTION

Any real physical systems are subject to noise due to the inevitable coupling to the environment. It is important to understand the dynamics of quantum many-body systems under noise. Universal quantum circuits represent an important class of quantum many-body systems which are generic in the sense that they can simulate any other complicated quantum dynamics [1]. Understanding the computational power and the classical simulatability of noisy universal quantum circuits, therefore, poses a fascinating question of both fundamental interest and practical importance [2–6].

Direct simulation of noisy quantum many-body dynamics, which is typically described by an open system through the master equation [7, 8], is very challenging, more difficult than the simulation of the corresponding noiseless dynamics. On the other hand, it is known that the output of very noisy quantum circuits can be classically simulated efficiently, i.e., with a polynomial time cost, through an indirect method [9, 10]. If the noise is not at a very high level, what is the computational power of noisy quantum devices or systems? Whether is it possible to efficiently simulate their output or behavior using classical computers? These questions still remain unknown and they are of great practical importance: with the advent of the Noisy Intermediate-Scale Quantum (NISQ) era [6], most of the quantum systems that we have in the lab belong to this class where the noise per quantum gate (operation) is at a modest but non-negligible level.

In this paper, we address these questions by providing some stimulating results in this direction. We consider a large class of random universal quantum circuits under symmetric or asymmetric depolarization noise. For generic instances from this set of circuits, we prove that if the noise per quantum gate is at a constant level, the output of these quantum circuits can be classically efficiently simulated with the time cost polynomial in the system size. This result holds true even if a particular class of gates from the universal set are noiseless. For instance, we may assume all the Clifford gates are noiseless and non-Clifford single-bit gates (such as the  $\pi/8$ -gate from the universal gate set) have a constant level of error rate. This assumption is well motivated as the Clifford gates can be more conveniently protected from noise through fault-tolerant quantum error correction or topological computation [11–13]. For the proof, we develop a tensor network formalism [14, 15] to analyze the Fourier spectrum of the quantum circuits. The Fourier spectrum analysis [16] has been used recently for classical simulation of noisy quantum dynamics from the Ising interaction [17, 18]. Our developed tensor network formalism turns out to be particularly powerful to analyze the Fourier spectrum when we have a constant level of noise per gate which leads to independent block summation and efficient truncation in the Fourier space.

This result has some interesting implication on the pursuit of quantum supremacy demonstration [5, 19]. Conventional complexity theory arguments on quantum supremacy are for noiseless systems in the asymptotic limit [5, 19, 20], and in this case efficient classical simulation of certain quantum circuits will lead to collapse of the so-called polynomial hierarchy in the computational complexity classes under reasonable conjectures. The real systems will necessarily have noise and in this case the result here shows that in the asymptotic limit (meaning that the circuit depth goes to infinity) the output of the circuit is classically simulatable and actually approaches a uniform distribution for any constant level of error per gate. Recently, the approach to a uniform distribution has been supported with numerical evidence [21, 22]. Here, we give a rigorous analytic proof of the asymptotic distribution. This result suggests that in the case of noisy gates as for real experiments, the claim of quantum supremacy is not based on the complexity theory argument such as the collapse of the polynomial hierarchy, which is defined in the asymptotic limit, but instead more based on the practical difficulty to simulate such quantum systems with classical computers for an intermediate depth

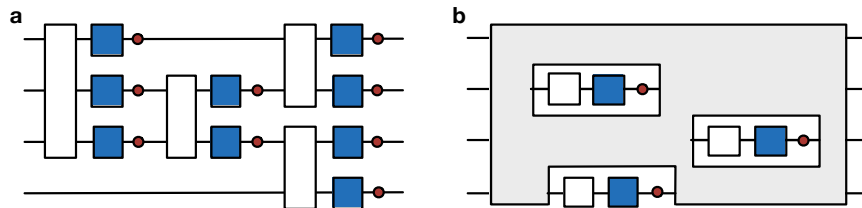


FIG. 1: **Two types of ensembles of noisy quantum circuits.** **a**, All the gates represented by blue boxes are chosen uniformly from the four possible Pauli matrices  $X^a Z^b$  with  $a, b = 0, 1$  (including the identity matrix with  $a = b = 0$ ). The gates represented in white could be any gates in the universal gate set. The red circles represent the channel of noise that is specified in the main text. The depth  $d$  of this circuit is defined as the smallest number of blue boxes along any horizontal lines. **b**, The grey color box represents any circuits composed by noiseless Clifford gates. The white boxes represents non-Clifford gates, which are normally chosen as the single-bit  $\pi/8$ -gate for universal quantum computation. The non-Clifford gates are subject to the noise channel represented by the red boxes.

of the circuits (at certain intermediate depths of the circuits it is difficult to simulate the output classically by all the algorithms known so far, although in the limit of the infinite depth the output distribution is known and becomes uniform).

### SUMMARY OF THE MAJOR RESULTS

We model the error for each gate in the quantum circuit by a generalized type of depolarization noise. For a density operator  $\rho$ , the noise is modeled by a composition of Pauli errors  $\mathcal{E}_3 \circ \mathcal{E}_2 \circ \mathcal{E}_1(\rho)$ , where  $\mathcal{E}_i(\rho) \equiv (1 - \epsilon_i)\rho + \epsilon_i \sigma_i \rho \sigma_i$  and  $\sigma_1 = Z$ ,  $\sigma_2 = X$ ,  $\sigma_3 = Y$  represent the Pauli operators along the  $z, x, y$  directions. As shown in the Methods section, this error model allows arbitrary mixture of Pauli errors including the depolarizing noise. It is important to have at least two  $\epsilon_i$  nonzero for the noise model to be generic, and we denote the second largest  $\epsilon_i$  ( $i = 1, 2, 3$ ) as  $\epsilon$ , which is a key noise parameter for our following theorems. The noise channels are denoted as red circles in Fig. 1.

Instead of analyzing a specific circuit, we consider noisy quantum circuits randomly chosen from an ensemble and investigate what portions of the circuits in this ensemble can be efficiently simulated classically. Two types of circuit ensembles are illustrated in Fig. 1. In Fig. 1a, we consider an ensemble where all the gates are subject to noise. To describe this ensemble, for each output qubit of arbitrary quantum gates, we apply a single-bit operation randomly chosen from the set of Pauli matrices  $\{X^{y_2} Z^{y_1}\}_{y_1, y_2}$ , where the indices  $y_1, y_2$  with values of 0, 1 are uniformly chosen from the four possible combinations. We use the blue boxes in Fig. 1a to represent this random Pauli operation. After the Pauli operation, each qubit is subject to the noise channel which is denoted by the red circle in Fig. 1a. A specific quantum circuit in this ensemble therefore can be parameterized by the sequence of chosen indices denoted by the vector  $\mathbf{y} = \mathbf{y}_1 \mathbf{y}_2$ . In Fig. 1b, we consider an ensemble where part of the gates in the circuit, denoted by the grey block, are noise-free. The gate set in the grey-block by itself allows an efficient classical simulation. For instance, we may assume all the Clifford gates are perfect and thus in the grey block. This assumption is well motivated as the Clifford gates are easier to be protected from noise by quantum error correction [11] or topological computation [12, 13] and the set of Clifford gates can be efficiently simulated classically [23]. Non-Clifford gates for universal quantum computation, such as the T-gates ( $\pi/8$ -rotations), are subject to noise after the random Pauli operation, and they are denoted by the white squares in Fig. 1b.

Our major results are summarized by the following two theorems. The first theorem applies to the circuit ensemble represented by Fig. 1a where each gate is subject to noise.

**Theorem 1** Consider the ensemble of noisy quantum circuits represented by Fig. 1a with circuit depth  $d$  and measurement in any local basis on either a constant number of qubits or all the  $n$  qubits with the ensemble satisfying the anti-concentration condition. For at least  $1 - \eta$  fraction of the circuits in the ensemble with  $\eta = e^{-2\epsilon d}$ , the output distribution from the measurement is approximately a uniform distribution with additive error smaller than  $\delta = c e^{-\epsilon d}$ , where  $c$  is a constant independent of  $n, d$  and  $\epsilon$ .

In the above theorem, we assume the anti-concentration condition when we consider the distribution of all the qubits, which is a standard assumption in the literature on quantum supremacy [5, 19, 21, 24–26]. Roughly speaking, this condition means that the population is distributed over the whole Hilbert space of  $2^n$ -dimensions and no components dramatically stand out among the  $2^n$  possibilities. The precise statement is specified in the Methods section. Theorem

1 means that when all the gates are subject to noise of a depolarization nature, almost all the circuits (except for an exponentially small fraction) will lead to nearly uniform distributions (with exponentially small additive errors) for the measured qubits when  $\epsilon d$ , the product of the gate error rate and the circuit depth, is large enough.

Our second theorem applies to the ensemble shown in Fig. 1b where part of the gates in the circuit are noise free. In this case, the output distribution is far from being uniform, however, it can still be classically simulated within a polynomial time by the following theorem:

**Theorem 2** Consider the ensemble of quantum circuits shown in Fig. 1b and measurement on a constant number of qubits. For at least  $1 - \eta$  fraction of the circuits in this ensemble, there exists a classical algorithm to approximate the output probability of the noisy circuits with additive error bounded by  $\delta$  which runs in polynomial time

$$\text{poly}(n) \cdot (8m)^{l(\epsilon, \delta, \eta)}, \quad (1)$$

where  $m$  is the number of noisy gates,  $\text{poly}(n)$  comes from the simulation cost of noiseless part of the circuit and

$$l(\epsilon, \delta, \eta) \approx \ln(2^r \delta^{-1} (1 + \sqrt{\eta^{-1}})) / 2\epsilon, \quad (2)$$

where  $r$  is the number of qubits being measured and  $\epsilon, \delta, \eta$  can be any positive constants.

Theorem 2 implies that many nontrivial quantum circuits can be efficiently simulated classically. For instance, even when all the gates are perfect in the universal gate-set except for the single-bit T gate, which is subject to a small constant level of error rate, most of universal quantum circuits composed by these gates are classically simulatable except for an arbitrarily small constant fraction of subsets. This result is quite surprising and it has seemingly contradiction with the threshold theorem for fault-tolerant quantum computation, where we know that the gates below a small constant level of error rate (threshold) are capable for reliable universal quantum computing. The result here is actually consistent with the threshold theorem: it shows generic quantum circuits (except for a  $\eta$ -small subset) are classically simulatable under a constant level of error rate per physical gate. Fault-tolerant quantum error correction requires a particular circuit structure of physical gates for its implementation, which is non-generic in the space of all randomly chosen quantum circuits and belongs to the exceptional small subset that cannot be efficiently simulated classically. If one takes the logic gates as the basic unit of the circuits, universal quantum computation means that we can of course realize any generic quantum circuits of logic qubits. The error rate per logic qubit, however, is not a constant but required to approach zero inversely with the system size, so again it is outside of the application region of our theorems here for classical simulatability. Therefore, our result has no contradiction with the threshold theorem. Instead, it reveals the subtle boundary between classical simulatability and the power of quantum computing: although generic noisy quantum circuits are classically simulatable as indicated by the theorems here, the fault-tolerant quantum error correction implements a particular (non-generic) type quantum circuit of physical gates that escapes the curse of noise and thus is essential for the power of quantum computing.

The proof of our theorems has three steps: First, we develop the tensor network tool to represent the ensemble of noisy quantum circuits and their Fourier spectrum. Second, we show that the probability distribution from measurement on the final state can be written as a sum of Fourier series, where the noise in quantum gates leads to exponential decay of the terms in this series, so a good approximation can be obtained by truncating the series. Finally, we show that the tensor network representation of the Fourier spectrum of quantum circuits breaks into separable pieces, which makes it possible to efficiently calculate the Fourier series and their summation. The following three sections are devoted to detailed explanations of the above three steps one by one. For theorems 1 and 2 with different circuit ensembles, the proofs only differ in the last step. For simplicity of the notation, we focus on the noise model  $\mathcal{E}_2 \circ \mathcal{E}_1$  for the proof in the main text. The more general noise model is discussed in the Methods section.

## TENSOR NETWORK REPRESENTATION OF NOISY QUANTUM CIRCUITS

Each particular sample from the quantum circuit ensemble considered in Theorem 1 or 2 is described by the bit string  $\mathbf{y}_1 \mathbf{y}_2$  of  $2m$  bits, representing the sequential choice of the Pauli matrices, where  $m$  denotes the total number of noisy gates in the circuit. For this particular circuit, if we measure  $r$  output qubits, the conditional output distribution can be described as  $q_{\mathbf{x}|\mathbf{y}_1 \mathbf{y}_2} = q_{\mathbf{x}, \mathbf{y}_1 \mathbf{y}_2} / q_{\mathbf{y}_1 \mathbf{y}_2}$ , where  $\mathbf{x}$  denotes the bit string of  $r$  measured qubits, and  $q_{\mathbf{x}, \mathbf{y}_1 \mathbf{y}_2}$  ( $q_{\mathbf{y}_1 \mathbf{y}_2}$ ) denotes respectively the joint output distribution (the marginal probability to choose this circuit). In our case, the Pauli matrix indices  $\mathbf{y}_1 \mathbf{y}_2$  are chosen uniformly for the ensemble, so  $q_{\mathbf{y}_1 \mathbf{y}_2} = 2^{-2m}$ . If all the gates are perfect (in the case of  $\epsilon = 0$ ), the ideal unitary transformation represented by the whole quantum circuit is denoted by  $U_{\mathbf{y}_1 \mathbf{y}_2}$ . With



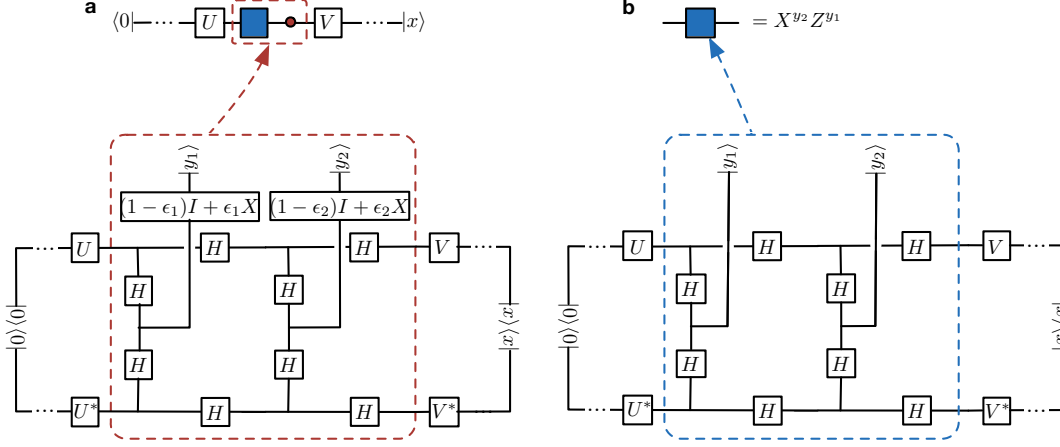


FIG. 3: **Tensor network representation of the basic units of noisy quantum circuits.** **a**, Representation of the Pauli matrix ensemble (the blue box) followed by the noise channel (the red dot). The blue box denotes the ensemble of gates  $\{X^{y_2}Z^{y_1}\}$  with  $y_1, y_2$  chosen randomly from  $\{0, 1\}$  with equal probability. The red dot denotes the noise channel  $\mathcal{E}_x(\mathcal{E}_z(\rho))$ , a combination of phase flip and bit-flip errors. The tensor network representation of this noise channel is derived from Fig. 2e by noticing that the additional bit flip channel is obtained through the Hadamard transformation  $H$  with  $HZH = X$  and  $H\mathcal{E}_z(Z^y\rho Z^y)H = \mathcal{E}_x(X^y H\rho H X^y)$ . We assume the noisy quantum circuit starts at an initial state denoted as  $|0\rangle$  and ends with a measurement in the computational basis  $|x\rangle$ , and the contraction of the tensor network gives the joint probability distribution  $q'_{x,y_1,y_2}$ . **b**, Representation of the noiseless Pauli matrix ensemble (the blue box only). Contraction of the tensor network in this case gives the joint probability distribution  $q_{x,y_1,y_2}$  for the corresponding noiseless circuit.

some basic notations of tensor network units and their composition rules. As a noiseless quantum circuit is composed of elementary unitary gates, it is straightforward to represent the distribution  $q_{x,y_1,y_2}$  with a tensor network. Different from  $q_{x,y_1,y_2}$ , to represent  $q'_{x,y_1,y_2}$ , we also need to have a tensor network representation of the dephasing and the bit flip error channels. Using the tensor network diagrammatic method, we derive in Fig. 2d and 2e the representation for the dephasing error channel  $\mathcal{E}_1(Z^y\rho Z^y)$  ( $y = 0, 1$ ). Similarly, with additional Hadamard gates, we have a tensor network representation for the bit flip error channel. The noise in our circuit can be composed from these basic units. In Fig. 3, we show the tensor network representation of the random gate set  $X^{y_2}Z^{y_1}$  (Fig. 3b) as well as this gate set followed by a noise channel  $\mathcal{E}_2 \circ \mathcal{E}_1$  (Fig. 3a). By the composition of these units, we get the representation for the probability distribution  $q'_{x|y_1,y_2}$ .

## FOURIER ANALYSIS OF NOISY QUANTUM CIRCUITS AND ITS TENSOR NETWORK REPRESENTATION

Each sample from the ensemble of noisy quantum circuits depends on a sequence of binary variables  $\mathbf{y} \equiv \mathbf{y}_1\mathbf{y}_2$  that specify its choice of Pauli gates. For the probability distributions  $q_{x,y_1,y_2}$  and  $q'_{x,y_1,y_2}$ , one can define a binary Fourier transformation with respect to their  $\mathbf{y}$  variables as follows [16, 17]:

$$\begin{aligned} \hat{q}_{\mathbf{x},\mathbf{s}_1\mathbf{s}_2} &= \frac{1}{2^m} \sum_{\mathbf{y}} (-1)^{\mathbf{s} \cdot \mathbf{y}} q_{x,y_1,y_2}, \\ q_{x,y_1,y_2} &= \frac{1}{2^m} \sum_{\mathbf{s}} (-1)^{\mathbf{s} \cdot \mathbf{y}} \hat{q}_{\mathbf{x},\mathbf{s}_1\mathbf{s}_2}, \end{aligned} \quad (5)$$

where  $\mathbf{s} = \mathbf{s}_1\mathbf{s}_2$  of  $2m$  bits are the dual variables of  $\mathbf{y} = \mathbf{y}_1\mathbf{y}_2$  and  $\mathbf{s} \cdot \mathbf{y} = \mathbf{s}_1 \cdot \mathbf{y}_1 + \mathbf{s}_2 \cdot \mathbf{y}_2$  denotes the binary inner product. The Fourier transformation  $\hat{q}'_{\mathbf{x},\mathbf{s}_1\mathbf{s}_2}$  is defined in the same way. An important observation here is that the binary Fourier transformation has a very natural tensor network representation as shown in Fig. 4a. By identifying the variables of a boolean function as tensor indices, the binary Fourier transformation is simply contraction with the Hadamard matrices, which is also known as the Walsh-Hadamard transformation.

Using the tensor network representation of the binary Fourier transformation, it is easy to see a relation between  $\hat{q}'_{\mathbf{x},\mathbf{s}_1\mathbf{s}_2}$  and  $\hat{q}_{\mathbf{x},\mathbf{s}_1\mathbf{s}_2}$  by contraction with the noise matrix  $(1 - \epsilon_{1,2})I + \epsilon_{1,2}X$  as shown in Fig. 4b. We get an important

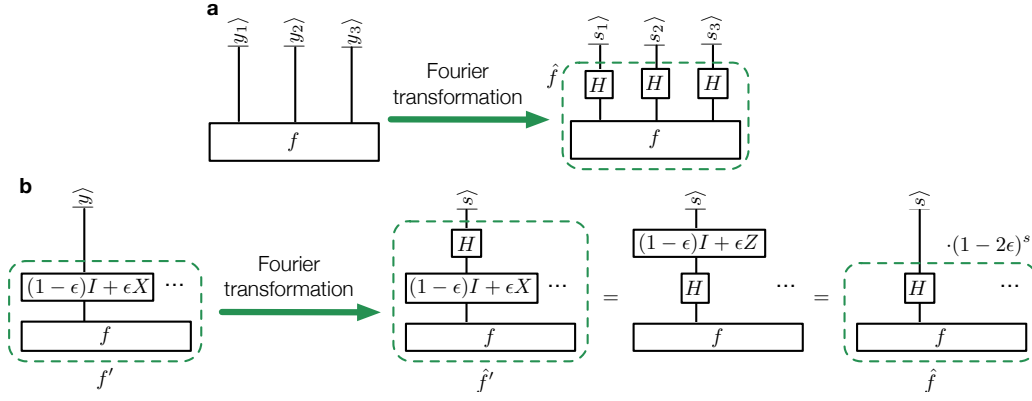


FIG. 4: **Tensor network representation of Fourier transformation of noisy quantum circuits.** **a**, Tensor Representation of Fourier transformation on boolean variables  $y_i$ , which is equivalent to the Hadamard transformation on the corresponding indices. The inverse Fourier transformation is the same because of  $H^2 = I$ . **b**, Representation of the Fourier transformation on noisy circuits. As  $HXH = Z$  and  $[(1 - \epsilon)I + \epsilon Z]|s\rangle = (1 - 2\epsilon)^s|s\rangle$ , we immediately get that the Fourier spectrum of the noisy circuit is related to the spectrum of the noiseless circuit by a simple multiplication factor  $(1 - 2\epsilon)^s$ .

property [16, 17]

$$\begin{aligned} \hat{q}'_{\mathbf{x}, \mathbf{s}_1 \mathbf{s}_2} &= (1 - 2\epsilon_1)^{|\mathbf{s}_1|} (1 - 2\epsilon_2)^{|\mathbf{s}_2|} \hat{q}_{\mathbf{x}, \mathbf{s}_1 \mathbf{s}_2} \\ &\simeq e^{-2(\epsilon_1 |\mathbf{s}_1| + \epsilon_2 |\mathbf{s}_2|)} \hat{q}_{\mathbf{x}, \mathbf{s}_1 \mathbf{s}_2} \end{aligned} \quad (6)$$

where  $|\mathbf{s}_{1,2}|$  denotes the Hamming weight of the bit string  $\mathbf{s}_{1,2}$ , i.e., the number of 1s in  $\mathbf{s}_{1,2}$ . So the noise in gates makes the Fourier components exponentially decay with  $|\mathbf{s}_{1,2}|$ , which suggests that the summation can be approximated by truncating the Fourier series under noisy gates.

We define the pseudo probability  $p'_{\mathbf{x}, \mathbf{y}_1 \mathbf{y}_2}$  through truncating the Fourier series of  $\hat{q}'_{\mathbf{x}, \mathbf{y}_1 \mathbf{y}_2}$  to the Hamming weight  $l$  with  $\hat{p}'_{\mathbf{x}, \mathbf{s}_1 \mathbf{s}_2} = \hat{q}'_{\mathbf{x}, \mathbf{s}_1 \mathbf{s}_2}$  if  $|\mathbf{s}_1| + |\mathbf{s}_2| < l$  and  $\hat{p}'_{\mathbf{x}, \mathbf{s}_1 \mathbf{s}_2} = 0$  otherwise. Assuming each  $\hat{p}'_{\mathbf{x}, \mathbf{s}_1 \mathbf{s}_2}$  can be efficiently computed classically within a time  $t$  (we will prove this in the next section), then computing  $p'_{\mathbf{x}, \mathbf{y}_1 \mathbf{y}_2}$  through the Fourier inverse transformation is  $t(2m)^l$  since there are at most  $(2m)^l$  non-zero terms in the summation. The quantity we need is  $q'_{\mathbf{x}|\mathbf{y}_1 \mathbf{y}_2} = 4^m q'_{\mathbf{x}, \mathbf{y}_1 \mathbf{y}_2}$ , which is approximated by  $p'_{\mathbf{x}|\mathbf{y}_1 \mathbf{y}_2} = 4^m p'_{\mathbf{x}, \mathbf{y}_1 \mathbf{y}_2}$ . To quantify this approximation, we use the additive error defined as  $\delta_{\mathbf{y}_1 \mathbf{y}_2} \equiv \sum_{\mathbf{x}} |p'_{\mathbf{x}|\mathbf{y}_1 \mathbf{y}_2} - q'_{\mathbf{x}|\mathbf{y}_1 \mathbf{y}_2}|$ . Instead of analyzing each individual  $\delta_{\mathbf{y}_1 \mathbf{y}_2}$ , we analyze the average behavior through the expectation value  $\delta_0 \equiv \mathbb{E}_{\mathbf{y}_1 \mathbf{y}_2} [\delta_{\mathbf{y}_1 \mathbf{y}_2}]$  and the variance  $\Delta \equiv \sqrt{\mathbb{E}_{\mathbf{y}_1 \mathbf{y}_2} [\delta_{\mathbf{y}_1 \mathbf{y}_2}^2] - \delta_0^2}$ , where  $\mathbf{y}_1 \mathbf{y}_2$  are chosen from the uniform distribution. By direct calculation shown in the Methods section, we find that

$$\delta_0 \leq ce^{-2\epsilon l}, \quad \Delta \leq ce^{-2\epsilon l}, \quad (7)$$

where  $\epsilon = \min(\epsilon_1, \epsilon_2)$  and  $c$  is a constant. By using the Chebyshev inequality, we can then bound  $\delta_{\mathbf{y}_1 \mathbf{y}_2} \leq \delta$  for at least  $1 - \eta$  fraction of  $\mathbf{y}_1 \mathbf{y}_2$  as long as  $\eta(\delta - \delta_0)^2 \leq \Delta^2$ . By choosing arbitrarily small  $\eta$  and  $\delta$ , we conclude that almost all  $\delta_{\mathbf{y}_1 \mathbf{y}_2}$  are well bounded and the approximation is valid for most of the random quantum circuits.

## PROOF OF THEOREMS THROUGH ANALYZING THE FOURIER SPECTRUM

Through the above analysis, we reduce the problem of calculating the conditional distribution  $q'_{\mathbf{x}|\mathbf{y}_1 \mathbf{y}_2}$  to computing the Fourier spectrum  $\hat{q}_{\mathbf{x}, \mathbf{s}_1 \mathbf{s}_2}$ . To prove theorems 1 and 2, the remaining task is to find a method to efficiently compute  $\hat{q}_{\mathbf{x}, \mathbf{s}_1 \mathbf{s}_2}$ . In Fig. 5, using the diagrammatic method, we derive the tensor network representation of the Fourier spectrum  $\hat{q}_{\mathbf{x}, \mathbf{s}_1 \mathbf{s}_2}$ . The final representation is shown in Fig. 5a, with the derivation steps illustrated in Fig. 5(b-d). The tensor network representation of  $\hat{q}_{\mathbf{x}, \mathbf{s}_1 \mathbf{s}_2}$  shows a crucial property: it breaks into separable pieces at every places of the random Pauli gates. This property allows us to efficiently calculate the Fourier spectrum  $\hat{q}_{\mathbf{x}, \mathbf{s}_1 \mathbf{s}_2}$  for the whole circuit.

First, we prove Theorem 1 by calculating the Fourier spectrum  $\hat{q}_{\mathbf{x}, \mathbf{s}_1 \mathbf{s}_2}$  for the ensemble of the noisy circuits shown in Fig. 1a. The Fourier component  $\hat{q}_{\mathbf{x}, \mathbf{s}_1 \mathbf{s}_2}$  breaks into product of many independent fragments, separated by the blue boxes shown in Fig. 6a (see also Figs. 1a, 3a, and 5a for the representation). This product is nonzero if and only if

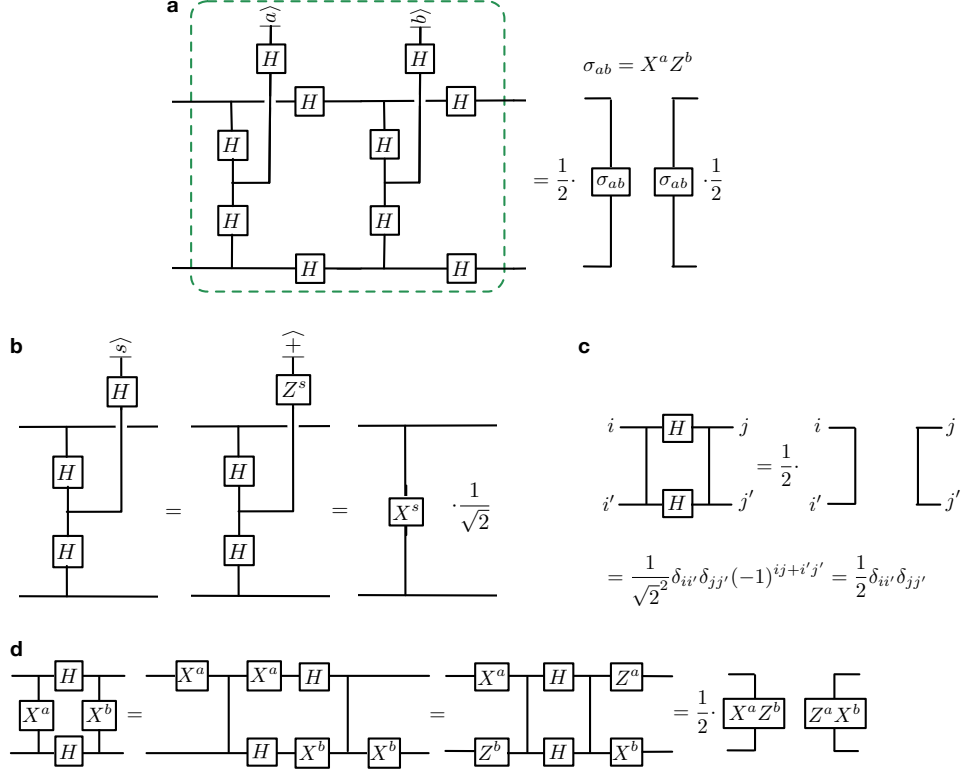


FIG. 5: **Separability for the Tensor network representation of the Fourier spectrum of quantum circuits.** **a**, The pivotal property of separability for the Fourier spectrum, which shows that the Fourier transformation of the Pauli ensemble (the basic unit denoted by the blue box in Fig. 3b) on the left side can be written as a product of two separable tensor networks on the right side, where  $\sigma_{ab}$  denotes the matrix  $X^a Z^b$ . This separability is derived in Figs. **b-d** through the diagrammatic method. The separability is the key to simplification of the calculation of the Fourier spectrum for ensembles of large quantum circuits. **b**, Step 1 to derive the separability which uses the equalities in Fig. 2c. **c**, Step 2 to derive the separability in the case with  $a = b = 0$ . **d**, Step 3 to derive the separability for the general case with arbitrary  $a, b$ . We have used the result of Fig. 5b and the tensor property in Fig. 2c.

all the fragments are nonzero. The fragment of a single-bit gate is shown in Fig. 6a. To make this fragment nonzero, if  $\sigma_{ab} = I$  (i.e., the dual variables  $a = b = 0$  in the Fourier index  $\mathbf{s}_1 \mathbf{s}_2$ ), we should also have  $\sigma_{cd} = I$ . Similarly, as shown in Fig. 6b, to make the Fourier fragment of an entangling gate nonzero, if  $\sigma_{ab} = \sigma_{a'b'} = I$ , we have to choose  $\sigma_{cd} = \sigma_{c'd'} = I$ . Using this property, we can prove that the Fourier spectrum  $\hat{q}_{\mathbf{x}, \mathbf{s}_1 \mathbf{s}_2} = 0$  for all the components  $\mathbf{s}_1 \mathbf{s}_2$  with  $0 < |\mathbf{s}_1| + |\mathbf{s}_2| < d$ . To prove this, we cut the circuit in Fig. 1a into  $d$  vertical layers, where  $d$  is the circuit depth. If we have the Fourier index  $|\mathbf{s}_{1i}| + |\mathbf{s}_{2i}| = 0$  for any  $i$ th layer (corresponding to choice of the  $I$  matrix for all the cuts in this layer), with the property shown in Fig. 6a and 6b, we have to choose  $|\mathbf{s}_{1j}| + |\mathbf{s}_{2j}| = 0$  for all the other layers  $j$  to make the product  $\hat{q}_{\mathbf{x}, \mathbf{s}_1 \mathbf{s}_2}$  nonzero (otherwise one of its Fourier fragments will be zero). So, to make  $\hat{q}_{\mathbf{x}, \mathbf{s}_1 \mathbf{s}_2}$  nonzero, we either have the Hamming weight  $|\mathbf{s}_1| + |\mathbf{s}_2| = 0$ , or have  $|\mathbf{s}_{1i}| + |\mathbf{s}_{2i}| > 0$  for each of the  $d$  layers which means  $|\mathbf{s}_1| + |\mathbf{s}_2| \geq d$ . This proves the above statement.

To finish the proof of theorem 1, we just need to take  $l = d$  in Eq. (7). This leads to  $\hat{p}'_{\mathbf{x}, \mathbf{s}_1 \mathbf{s}_2} = 0$  for  $|\mathbf{s}_1| + |\mathbf{s}_2| > 0$ , which gives a uniform distribution  $p'_{\mathbf{x}|\mathbf{y}_1 \mathbf{y}_2}$  after the Fourier transformation. In combination with the Chebyshev inequality, we thus have proved theorem 1 by choosing  $\delta \sim e^{-\epsilon d} \gg \delta_0 \sim e^{-2\epsilon d}$ .

Now we prove theorem 2 by considering the ensemble of noisy quantum circuits shown in Fig. 1b. The Fourier spectrum of this circuit is illustrated in Fig. 6c, where the grey part denotes the Clifford gates. The Fourier circuit breaks up at each place of the non-Clifford gates (the white and blue boxes in Fig. 2a), but due to the connection by the Clifford gates, it does not break into independent pieces. In Fig. 6c, we write the matrix at the breaking points into an equivalent Clifford gates. So the whole circuit for the Fourier spectrum becomes almost Clifford except for the non-Clifford gates (white boxes) at the breaking points. We can decompose the non-Clifford gates into a summation of  $4^l$  terms where each term is a tensor product of Pauli matrices. Only  $l$  white boxes have non-trivial effect because the non-Clifford gate  $U$  in Fig. 6c cancels through  $U^\dagger I U = I$  if the corresponding dual variables in  $\mathbf{s}_1 \mathbf{s}_2$  are both 0

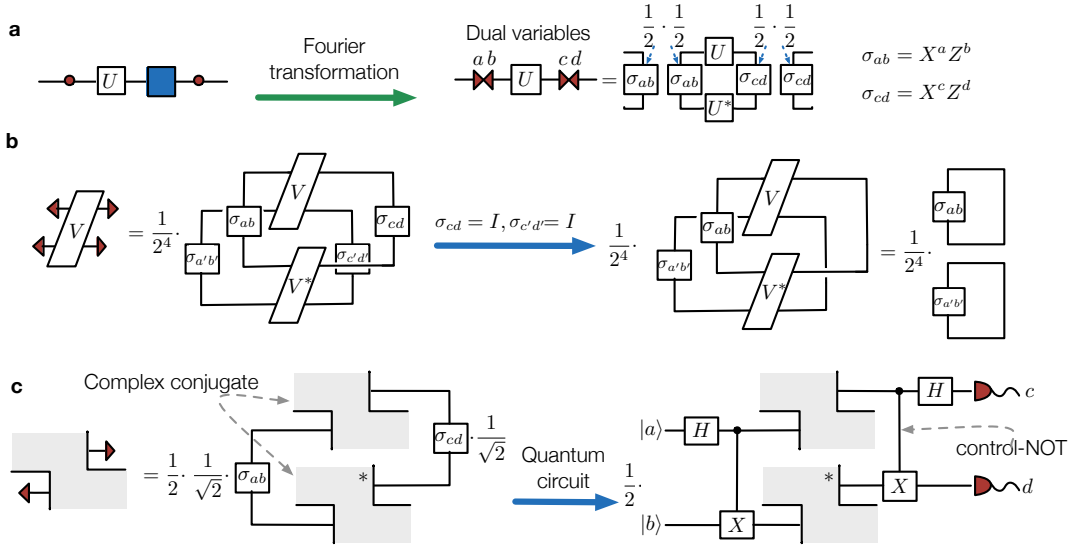


FIG. 6: **The computing rule for the Fourier spectrum through the tensor network representation.** **a**, The computing rule for the Fourier spectrum of noisy quantum circuits: after the transformation, the tensor network breaks into two separated pieces at the position of the basic unit of Pauli ensemble (the blue box and the red dot), so we denote the breaking point by the two red triangles, which correspond to a product of the tensor networks shown on the right side. **b**, An important property for contraction of the tensor network used for proof of Theorem 1. When we contract a piece of tensor network with an arbitrary two-qubit gate  $V$  in the between, if  $\sigma_{cd} = \sigma_{c'd'} = I$  on one side of the network, the contraction leads to a tensor network shown on the right side which is proportional to  $\text{tr} \sigma_{ab} \cdot \text{tr} \sigma_{a'b'}$  and non-zero only when  $\sigma_{ab} = \sigma_{a'b'} = I$ . **c**, A property of the tensor network used for proof of Theorem 2. The grey part represents any Clifford quantum circuits and the lower grey part denotes the complex conjugate of the upper one. The matrices  $\sigma_{ab}$  and  $\sigma_{cd}$  can be represented as the Clifford gates (the Hadamard  $H$  and the CNOT gate) acting on the computational basis-vectors  $|a\rangle, |b\rangle$  (on the left) or measured in the computational basis  $|c\rangle, |d\rangle$  (on the right). The whole equivalent circuit shown on the right figure is then of Clifford type and can be efficiently simulated classically.

(i.e.,  $a = b = 0$  in Fig. 6c). The Fourier spectrum is therefore expressed as a summation of a constant number ( $4^l$ ) of Clifford circuits, and by the Gottesman-Knill theorem [23], each Clifford circuits can be efficiently simulated.

To count the time complexity of computing  $\hat{p}'_{\mathbf{x}_1|\mathbf{y}_1\mathbf{y}_2}$ , suppose we truncate the Fourier series to the Hamming weight  $l$ . The time complexity of computing each Fourier component is  $4^l t$ , where  $4^l$  originates from the Pauli decomposition of the non-Clifford gates as we have discussed above and  $t = \text{poly}(n)$  is the time complexity of computing the remaining Clifford circuits. Then there are at most  $(2m)^l$  terms to be summarized, so the time complexity is  $\text{poly}(n)(8m)^l$ . Given the required precision of the output  $1 - \delta$  and the probability of failure  $\eta$ , we have  $\delta \lesssim \Delta/\sqrt{\eta} + \delta_0 \lesssim (1 + 1/\sqrt{\eta})ce^{-2\epsilon l}$  according to the Chebyshev inequality, where  $c = \sqrt{2^r}$  is a constant and  $r$  is the number of qubits being measured. This requires  $l \approx \ln(c\delta^{-1}(1 + \sqrt{\eta^{-1}}))/2\epsilon$ , which gives the expression in theorem 2. This completes the proof of the theorem 2.

## SUMMARY AND OUTLOOK

In summary, we have proved that most of noisy quantum circuits can be efficiently simulated classically under any constant level of error rate per gate. The result holds even if a subset of quantum gates, such as all the Clifford gates, can be done perfectly. The seemingly contradiction between this surprising result and the threshold theorem for fault tolerant quantum computation is resolved by noting that the quantum error correction circuit is required to be highly structured and thus may take only a zero-measure subspace under random choice of quantum circuits. The theorems derived in this paper show that for noisy quantum circuits the dividing lines between classical simulatability, quantum supremacy, and universal quantum computing are very subtle. What are the characteristic features of noisy quantum circuits to make them either classically simulatable or noise-resilient for universal quantum computing? It remains an important open question and further studies along this line will surely deepen our understanding of the power and limitation of quantum computation.

To prove our theorems, we have developed a powerful tool based on tensor network representation of noisy quantum circuits and their measurement outcomes. We discover that the tensor network representation of the Fourier spectrum of quantum circuits always breaks into many independent pieces. This separability of its Fourier spectrum is a surprising and nice property, which greatly simplifies our analyses of complicated dynamics of quantum circuits. Besides its use in analyzing the structure of large-scale quantum circuits, this property of separable Fourier spectrum may find applications in other fields, such as for understanding of many-body quantum dynamics under open environments [2–4], a key problem on the physics frontier.

## METHODS

### Noise model

We can simulate the more general noise model from an arbitrary mixture of Pauli errors

$$\mathcal{E}(\rho) = (1 - \epsilon_x - \epsilon_y - \epsilon_z)\rho + \epsilon_x X\rho X + \epsilon_y Y\rho Y + \epsilon_z Z\rho Z \quad (8)$$

by successively applying the noise channel  $\mathcal{E}_z$

$$(S \cdot H \cdot \mathcal{E}_z^{(3)} \cdot H \cdot S^\dagger) \circ (H \cdot \mathcal{E}_z^{(2)} \cdot H) \circ \mathcal{E}_z^{(1)}, \quad (9)$$

with

$$\mathcal{E}_z^{(i)}(\rho) = (1 - \epsilon_i)\rho + \epsilon_i Z\rho Z, \quad (10)$$

where  $\circ$  denotes composition of quantum channels,  $\cdot$  denotes matrix multiplication, and  $H$  ( $S$ ) denotes respectively the Hadamard (phase) gate. Since  $HZH = X$  and  $SHZHS^\dagger = Y$ , adjusting  $\epsilon_i$  will give any non-zero small  $\epsilon_{x,y,z}$  through the following relations

$$\begin{aligned} \epsilon_z &= \epsilon_1(1 - \epsilon_2)(1 - \epsilon_3) + (1 - \epsilon_1)\epsilon_2\epsilon_3; \\ \epsilon_x &= \epsilon_2(1 - \epsilon_1)(1 - \epsilon_3) + (1 - \epsilon_2)\epsilon_1\epsilon_3; \\ \epsilon_y &= \epsilon_3(1 - \epsilon_1)(1 - \epsilon_2) + (1 - \epsilon_3)\epsilon_1\epsilon_2. \end{aligned} \quad (11)$$

The value of the Jacobian determinant for the above transformation is

$$(2\epsilon_1 - 1)(2\epsilon_2 - 1)(2\epsilon_3 - 1). \quad (12)$$

According to the inverse function theorem, the solution always exists when  $\epsilon_i \neq 1/2$  (the Jacobian is nonzero). For the general noise model, the blue box in Fig. 1 is replaced by

$$Y^{y_3} X^{y_2} Z^{y_1} \propto X^{y_3+y_2} Z^{y_3+y_1}. \quad (13)$$

### Anti-concentration condition

The precise statement of anti-concentration condition is as follows [5, 19, 21, 24–26]:

$$\mathbb{E}_{U \sim \mathcal{D}^m} \left[ \sum_{\mathbf{x}} p_{\mathbf{x}|U}^2 \right] \leq \alpha 2^{-n}, \quad (14)$$

where  $\mathcal{D}$  denotes a uniform distribution for each blue box chosen from the corresponding gate set,  $m$  is the number of blue boxes,  $\mathcal{D}^m$  denotes a joint distribution of  $m$  random variables chosen independently from  $\mathcal{D}$ ,  $p_{\mathbf{x}|U}$  is the probability getting measurement result  $\mathbf{x}$  for the circuit  $U$ ,  $n$  is the number of bits in the vector  $\mathbf{x}$ , and  $\alpha$  is a constant. A sufficient but not necessary condition to satisfy the anti-concentration condition is that the ensemble achieves a unitary 2-design which is believed to be common for rich enough ensembles [27–30].

*Bounds for truncating the Fourier series*

In the main text, we have given the approximation error of truncating Fourier series through the average value and variance, using the Chebyshev inequality to bound the error for most of the circuits in the ensemble. Here, we give the detailed derivation. In this analysis, we assume the anti-concentration condition to hold when we consider measurement on all the output qubits.

For the variance, we have

$$\begin{aligned} \Delta^2 &= \mathbb{E}_{\mathbf{y}}[\delta_{\mathbf{y}}^2] - \delta_0^2 \leq \mathbb{E}_{\mathbf{y}}[\delta_{\mathbf{y}}^2] \\ &= \frac{1}{2^{2m}} \sum_{\mathbf{y}} \left( \sum_{\mathbf{x}} |p'_{\mathbf{x}|\mathbf{y}} - q'_{\mathbf{x}|\mathbf{y}}| \right)^2 \\ &\leq \frac{2^r}{2^{2m}} \sum_{\mathbf{x}, \mathbf{y}} \left( p'_{\mathbf{x}|\mathbf{y}} - q'_{\mathbf{x}|\mathbf{y}} \right)^2 \end{aligned} \tag{15}$$

$$\begin{aligned} &= 2^{2m+r} \sum_{\mathbf{x}, \mathbf{y}} \left( p'_{\mathbf{x}, \mathbf{y}} - q'_{\mathbf{x}, \mathbf{y}} \right)^2 \\ &= 2^{2m+r} \sum_{\mathbf{x}, \mathbf{s}} \left( \hat{p}'_{\mathbf{x}, \mathbf{s}} - \hat{q}'_{\mathbf{x}, \mathbf{s}} \right)^2 \end{aligned} \tag{16}$$

$$\begin{aligned} &= 2^{2m+r} \sum_{\mathbf{x}, |\mathbf{s}_1| + |\mathbf{s}_2| \geq l} (1 - 2\epsilon_1)^{2|\mathbf{s}_1|} (1 - 2\epsilon_2)^{2|\mathbf{s}_2|} \hat{q}_{\mathbf{x}, \mathbf{s}_1 \mathbf{s}_2}^2 \\ &\leq 2^{2m+r} (1 - 2\epsilon)^{2l} \sum_{\mathbf{x}, \mathbf{s}} \hat{q}_{\mathbf{x}, \mathbf{s}}^2 \\ &= 2^{2m+r} (1 - 2\epsilon)^{2l} \sum_{\mathbf{x}, \mathbf{y}} \hat{q}_{\mathbf{x}, \mathbf{y}}^2 \\ &= (1 - 2\epsilon)^{2l} \frac{1}{2^{2m}} 2^r \sum_{\mathbf{x}, \mathbf{y}} q_{\mathbf{x}|\mathbf{y}}^2 \\ &= (1 - 2\epsilon)^{2l} \mathbb{E}_{\mathbf{y}} \left[ 2^r \sum_{\mathbf{x}} q_{\mathbf{x}|\mathbf{y}}^2 \right] \\ &\leq c^2 (1 - 2\epsilon)^{2l} \leq c^2 e^{-4\epsilon l}. \end{aligned}$$

If the number of measured qubits  $r$  is a constant, since  $\mathbb{E}_{\mathbf{y}} \left[ \sum_{\mathbf{x}} q_{\mathbf{x}|\mathbf{y}}^2 \right] \leq 1$ , we take  $c^2 = 2^r$  which is also a constant. If we measure on all the  $n$  qubits, i.e.,  $r = n$ , we assume the anti-concentration condition which means  $\mathbb{E}_{\mathbf{y}} \left[ \sum_{\mathbf{x}} q_{\mathbf{x}|\mathbf{y}}^2 \right] = \alpha 2^{-n}$ , so  $c^2 = \alpha$ , which is still a constant. The step of Eq. (16) holds as the Hadamard matrix is unitary which preserves the  $l_2$  norm or equivalently we use the Parseval theorem in the theory of Fourier analysis.

For the average value, let us consider its square:

$$\begin{aligned} \delta_0^2 &= \left( \frac{1}{2^{2m}} \sum_{\mathbf{y}} \sum_{\mathbf{x}} |p'_{\mathbf{x}|\mathbf{y}} - q'_{\mathbf{x}|\mathbf{y}}| \right)^2 \\ &\leq \frac{2^r}{2^{2m}} \sum_{\mathbf{x}, \mathbf{y}} \left( p'_{\mathbf{x}|\mathbf{y}} - q'_{\mathbf{x}|\mathbf{y}} \right)^2, \end{aligned}$$

which is the same as Eq. (15). So,  $\delta_0$  has the same bound as  $\Delta$ , given by  $ce^{-2\epsilon l}$ .

According to the Chebyshev inequality, the outside fraction/probability  $\eta$  is bounded by

$$\eta \equiv \Pr[\delta_{\mathbf{y}} > \delta] = \Pr[\delta_{\mathbf{y}} - \delta_0 > \delta - \delta_0] \leq \frac{\Delta^2}{(\delta - \delta_0)^2}. \tag{17}$$

By choosing

$$\delta = ce^{-\epsilon l} \gg \delta_0 \tag{18}$$

for sufficiently large  $l$ , we can bound  $\eta$  by

$$\eta \leq e^{-2\epsilon l}. \quad (19)$$

This gives the statement below Eq. (7) in the main text and the result in theorem 1 when we choose  $l = d$ .

- 
- [1] Lloyd, S. Universal quantum simulators. *Science* **273**, 1073 (1996).
- [2] Cirac, J. I. & Zoller, P. Goals and opportunities in quantum simulation. *Nature Physics* **8**, 264–266 (2012).
- [3] Georgescu, I. M., Ashhab, S. & Nori, F. Quantum simulation. *Rev. Mod. Phys.* **86**, 153–185 (2014).
- [4] Hauke, P., Cucchietti, F. M., Tagliacozzo, L., Deutsch, I. H. & Lewenstein, M. Can one trust quantum simulators? *Reports on Progress in Physics* **75**, 082401 (2012).
- [5] Harrow, A. W. & Montanaro, A. Quantum computational supremacy. *Nature* **549**, 203–209 (2017).
- [6] Preskill, J. Quantum Computing in the NISQ era and beyond (2018). ArXiv: 1801.00862.
- [7] Lindblad, G. On the generators of quantum dynamical semigroups. *Communications in Mathematical Physics* **48**, 119–130 (1976).
- [8] Gorini, V., Kossakowski, A. & Sudarshan, E. C. G. Completely positive dynamical semigroups of  $n$ -level systems. *Journal of Mathematical Physics* **17**, 821–825 (1976).
- [9] Buhrman, H. *et al.* New limits on fault-tolerant quantum computation. *Foundations of computer science* 411–419 (2006).
- [10] Kempe, J., Regev, O., Unger, F. & De Wolf, R. Upper bounds on the noise threshold for fault-tolerant quantum computing. *international colloquium on automata languages and programming* 845–856 (2008).
- [11] Gottesman, D. *Stabilizer codes and quantum error correction*. Ph.D. thesis, California Institute of Technology (1997).
- [12] Sarma, S. D., Freedman, M. & Nayak, C. Majorana zero modes and topological quantum computation. *npj Quantum Information* **1**, 15001 (2015).
- [13] Nayak, C., Simon, S. H., Stern, A., Freedman, M. & Sarma, S. D. Non-abelian anyons and topological quantum computation. *Reviews of Modern Physics* **80**, 1083 (2008).
- [14] Orus, R. A practical introduction to tensor networks: Matrix product states and projected entangled pair states. *Ann. Phys.* **349**, 117–158 (2014).
- [15] Biamonte, J. & Bergholm, V. Tensor networks in a nutshell. *arXiv preprint arXiv:1708.00006* (2017).
- [16] O’Donnell, R. *Analysis of boolean functions* (Cambridge University Press, 2014).
- [17] Bremner, M. J., Montanaro, A. & Shepherd, D. J. Achieving quantum supremacy with sparse and noisy commuting quantum computations. *Quantum* **1**, 8 (2017).
- [18] Yung, M.-H. & Gao, X. Can Chaotic Quantum Circuits Maintain Quantum Supremacy under Noise? (2017). ArXiv:1706.08913v1.
- [19] Lund, A. P., Bremner, M. J. & Ralph, T. C. Quantum sampling problems, BosonSampling and quantum supremacy. *npj Quantum Information* **3**, 15 (2017).
- [20] Preskill, J. Quantum computing and the entanglement frontier (2012). ArXiv:1203.5813v3, 1203.5813.
- [21] Boixo, S. *et al.* Characterizing quantum supremacy in near-term devices. *Nature Physics* **14**, 595 (2018).
- [22] Boixo, S., Smelyanskiy, V. N. & Neven, H. Fourier analysis of sampling from noisy chaotic quantum circuits (2017). ArXiv: 1708.01875.
- [23] Gottesman, D. The heisenberg representation of quantum computers. *arXiv preprint quant-ph/9807006* (1998).
- [24] Aaronson, S. & Arkhipov, A. The computational complexity of linear optics. In *Proceedings of the Forty-third Annual ACM Symposium on Theory of Computing, STOC ’11*, 333–342 (ACM, 2011).
- [25] Bremner, M. J., Montanaro, A. & Shepherd, D. J. Average-case complexity versus approximate simulation of commuting quantum computations. *Phys. Rev. Lett.* **117**, 080501 (2016).
- [26] Hangleiter, D., Bermejo-Vega, J., Schwarz, M. & Eisert, J. Anti-concentration theorems for schemes showing a quantum speedup (2017). ArXiv:1706.03786v2.
- [27] Gross, D., Audenaert, K. & Eisert, J. Evenly distributed unitaries: On the structure of unitary designs. *Journal of Mathematical Physics* **48**, 052104 (2007). <https://doi.org/10.1063/1.2716992>.
- [28] Dankert, C., Cleve, R., Emerson, J. & Livine, E. Exact and approximate unitary 2-designs and their application to fidelity estimation. *Phys. Rev. A* **80**, 012304 (2009).
- [29] Brandão, F. G. S. L., Harrow, A. W. & Horodecki, M. Local random quantum circuits are approximate polynomial-designs. *Communications in Mathematical Physics* **346**, 397–434 (2016).
- [30] Onorati, E. *et al.* Mixing properties of stochastic quantum Hamiltonians (2016). ArXiv: 1606.01914.

**Acknowledgements** We thank Ignacio Cirac, Soonwon Choi, Liang Jiang, Zhengfeng Ji, Zhaohui Wei, Mingji Xia, Mengzhen Zhang, Sirui Lu and Yihong Zhang for helpful discussions. This work was supported by the Ministry of Education and the National Key Research and Development Program of China (2016YFA0301902).

**Author contributions:** X.G. carried out the work under L.M.D.’s supervision. All the authors made substantial contributions to this work. The authors declare that they have no competing interests. Correspondence and requests for materials should be addressed to L.M.D. (lmduan@tsinghua.edu.cn) or X. G. (gaoxungx@gmail.com).